-- Supporting Information --

Conjugated Polymer Dots for Multiphoton Fluorescence Imaging

Changfeng Wu, Craig Szymanski, Zachary Cain, and Jason McNeill*

Department of Chemistry and Center for Optical Materials Science and Engineering Technologies, Clemson University, Clemson, SC 29634

1. Preparation and characterization of the CPdots

Aqueous dispersions of CPdots were prepared using a reprecipitation method. 10 mg of conjugated polymer was dissolved in 10 g of HPLC grade tetrahydrofuran (THF) by stirring overnight under inert atmosphere and the solution was filtered through a 1.6 micron filter in order to remove any insoluble material. Highly dilute 10 and 20 ppm solutions were prepared from the filtered solution. A 2 mL quantity of the dilute polymer/THF solution was added quickly to 8 mL of deionized water while sonicating the mixture to aid mixing. The resulting nanoparticle suspension was filtered through a 0.2 micron membrane filter in order to remove larger aggregates—typically several percent of the polymer formed larger aggregates during the reprecipitation process. The THF was removed by evaporation under vacuum, followed by an additional filtration step. The overall polymer loss due to filtration was less than 20%. The resulting nanoparticle dispersions are clear, with colors similar to those of the polymers in THF solution.

For the AFM measurements, one drop of the nanoparticle dispersion was placed on a freshly cleaned glass substrate. After evaporation of the water, the surface topography was imaged with an Ambios Q250 multimode AFM in AC mode. As indicated in Figure S1, the nanoparticle size can be controlled by the precursor solution: a lower concentration of conjugated polymer in the precursor solution results in smaller particles (~10 nm in diameter), while the higher concentration leads to larger particles (~20 nm in diameter). Other factors such as the rate of

addition were also observed to affect particle size. UV-Vis absorption spectra were recorded with a Shimadzu UV-2101PC scanning spectrophotometer using 1 cm quartz cuvettes. Fluorescence spectra were recorded using a commercial fluorometer (Quantamaster, PTI, Inc.). UV-Vis absorption spectra and fluorescence spectra of particles prepared with different diameters (10 nm and 20 nm) are nearly identical (Figure S2), indicating that particle diameter has a negligible impact on the spectroscopic properties of the nanoparticles.

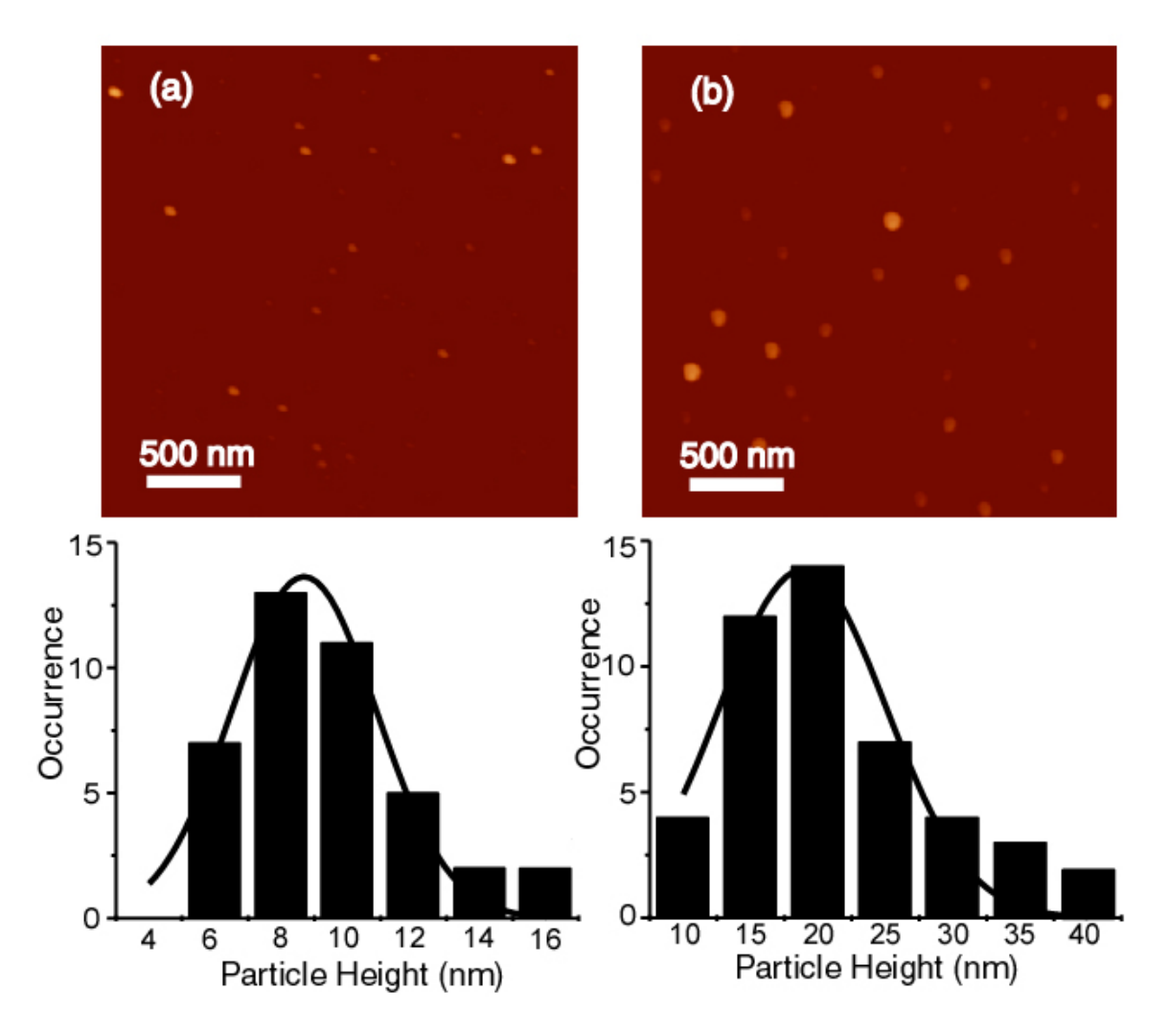


Figure S1 (a) A typical AFM image of PFPV dots prepared from 10 ppm precursor solution. Histogram of the particle height is shown in the bottom. (b) A typical AFM image of PFPV dots prepared from 20 ppm precursor solution. Histogram of the particle height is shown below each image.

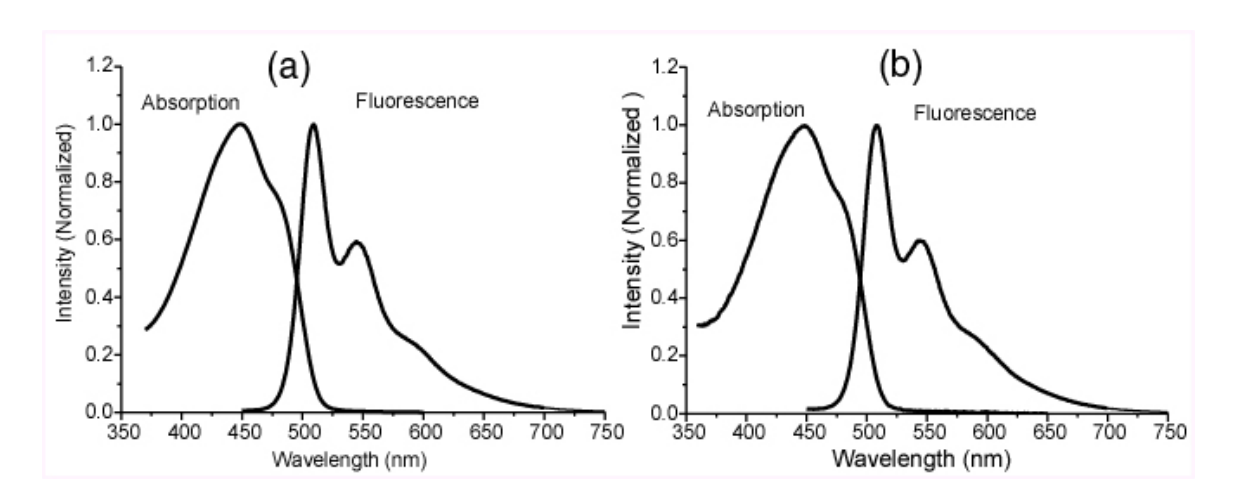


Figure S2 (a) Absorption and fluorescence spectra of the PFPV dots prepared from 10 ppm of precursor solution. (b) Absorption and fluorescence spectra of the PFPV dots prepared from 20 ppm of precursor solution.

2. Measurement of the two-photon action cross sections

The two-photon action cross-section, $\sigma_{2p}^* = \sigma_{2p} \varphi$, where σ_{2p} is the two-photon absorption cross-section and φ is the fluorescence quantum yield, is a quantitative measure of brightness for two-photon fluorescence applications. The two-photon action cross sections were determined as a function of wavelength using a home-built two-photon fluorescence spectrometer described as follows. A mode-locked, tunable Ti:sapphire laser (Coherent Mira 900) providing ~100 fs pulses at a repetition rate of 76 MHz was used as the light source for two-photon excitation. The laser beam was focused by a glass lens (f.l. = 30 mm) into a quartz cuvette containing an aqueous dispersion of CPdots. The two-photon excited fluorescence was collected in a perpendicular geometry using a 30 mm focal length lens, filtered by the combination of a Schott glass BG-38 filter and two 700 nm shortpass filters (Andover 700 FL07) in order to remove scattered laser light, and focused onto a single photon avalanche diode module (Perkin Elmer, SPCM-AQR). The count rate was determined using a 100 MHz bandwidth frequency counter (EZ Digital,

FC7015). Laser power was attenuated with a variable neutral density filter wheel and measured using a calibrated photodiode (Coherent LaserCheck).

Two-photon action cross-sections were obtained from the fluorescence data as follows. The time-averaged detected fluorescence photon flux F(t) can be expressed as

$$\langle F(t) \rangle \approx \frac{1}{2} \eta C \sigma_{2p}^* \frac{g_p}{f \tau} \frac{8n \langle P(t) \rangle^2}{\pi \lambda} ,$$
 (1)

where η is the fluorescence collection efficiency of the instrument; C is the fluorophore concentration; σ_{2p}^* is two-photon action cross section of the probe; g_p is a unitless factor related to pulse shape (0.66 for Gaussian laser pulse); f is the laser repetition rate; τ is the width (FWHM) of the laser pulse; n is the refractive index of the lens focusing the laser beam; λ is the laser wavelength; and $\langle P(t) \rangle$ is the average power of the laser. The factor $g_p/(f\tau)$ is approximately 10^5 for a Ti:sapphire laser with a 76 MHz repetition rate and $100 \, fs$ pulses. Only C and σ_{2p}^* are related to the sample, and all other parameters are constants, determined by the measurement system. Varying the laser power $\langle P(t) \rangle$ and recording the fluorescence intensity $\langle P(t) \rangle$ yields a quadratic dependence of fluorescence intensity on laser power. Plotting $Ln\langle F(t) \rangle$ vs $Ln\langle P(t) \rangle$ results in a straight line with slope of 2 and an intercept b, given by the expression,

$$b = Ln(\frac{1}{2}\eta C\sigma_{2p}^* \frac{g_p}{f\tau} \frac{8n}{\pi\lambda})$$
 (3)

Provided that a standard dye with known two-photon action cross-section is available, a relative determination of the two-photon action cross section of the species of interest is given by the expression,

$$\sigma_{2p}^* = \sigma_{2p,0}^* \frac{C_0}{C} \exp(b - b_0)$$
 (4)

where b and b_0 are obtained from log-log plots of laser intensity versus fluorescence intensity for the fluorophore of interest and the standard, respectively, and $\sigma_{2p,0}^*$ is the two-photon action cross-section of the standard. The above method was validated by determining the two photon action spectrum of rhodamine B using Lucifer yellow as a standard. The determined two photon action spectrum for rhodamine B is consistent with literature results for the absolute two-photon action cross-section. Figure S3 shows the log-log plot of the fluorescence intensities of the CPdots and rhodamine B solutions vs. the laser power at 800 nm wavelength. Fits to the experimental data yield a slope of 2.0 ± 0.1 , consistent with two-photon excited fluorescence. The sample concentrations were determined by UV-Vis spectrometry. The molar extinction coefficient used in determining the nanoparticle concentration is estimated using a previously described method based on AFM particle size measurements. $^{2.3}$

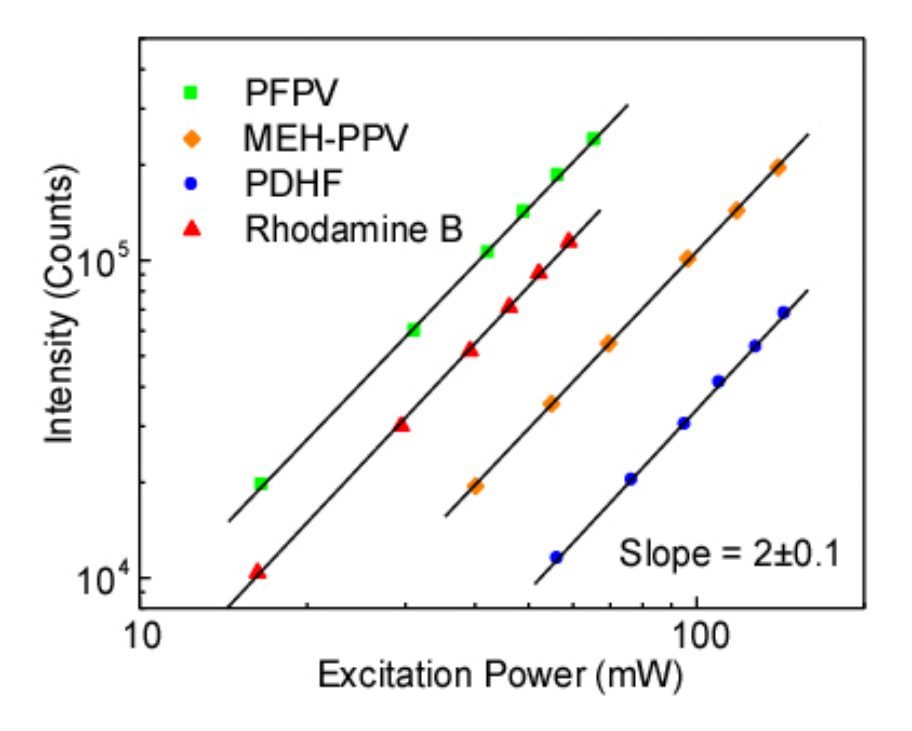


Figure S3 Two-photon fluorescence intensities vs. the excitation power for the rhodamine B and the CPdots. The sample concentrations determined from UV-Vis absorption are rhodamine $(1.00 \, \mu M)$, PFPV $(1.48 \, nM)$, MEH-PPV $(1.54 \, nM)$, and PDHF $(1.51 \, nM)$, respectively.

3. Single particle fluorescence imaging

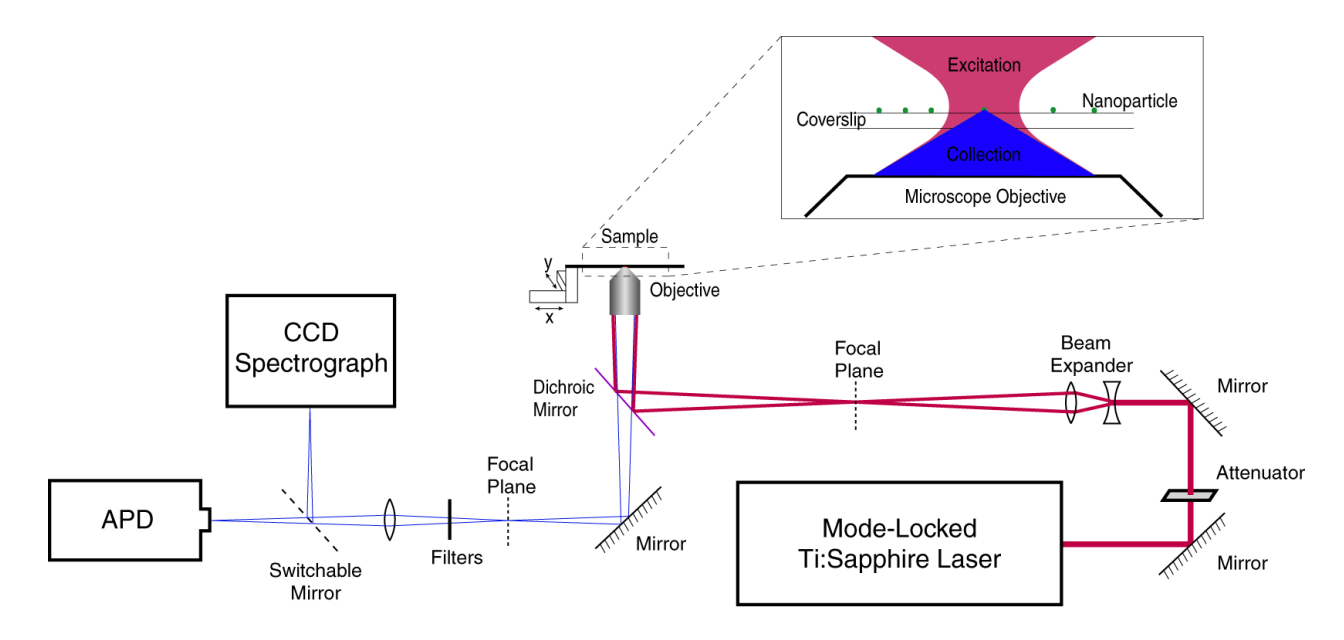


Figure S4 Experimental setup for single molecule spectroscopy.

Sample preparation for single particle two-photon fluorescence measurements consists of drop-casting a dilute CPdot suspension onto a cleaned microscope cover glass. Single particle two-photon fluorescence imaging was performed on a custom-built sample-scanning confocal microscope described as follows. The light source for two-photon imaging is a mode-locked Ti:sapphire laser (Coherent Mira 900) providing ~100 fs pulses at a repetition rate of 76 MHz and tunable from 770 to 870 nm. The laser beam is expanded and focused onto the focal plane of the epi-illumination port of an inverted fluorescence microscope (Olympus IX-71). Inside the microscope, the laser beam is reflected by a shortpass dichroic mirror (Chroma 675DCSX) towards the back of a high numerical aperture objective (Olympus Ach, 100X, 1.25 NA, Oil) and is focused to a nearly diffraction-limited spot. Fluorescence from CPdots is collected by the same objective lens and filtered by the combination of a BG-38 filter (Schott glass) and two 700 nm shortpass filters (Andover 700 FL07). The fluorescence is then focused onto a single photon avalanche diode module (Perkin Elmer, SPCM-AQR) and the fluorescence counts are recorded

using a 100 MHz counter card (NI-PCI-6602, National Instruments). The coverslip is mounted on a piezoelectric XYZ scanner (P-517.3CL, Polytec PI) connected to the analog outputs of a multifunction data acquisition card (NI-PCI-6036E, National Instruments). Images were acquired by raster scanning the sample under the control of custom data acquisition software written in the LabView environment (National Instruments). A schematic of the apparatus is shown in Figure S4. After an image is obtained, a particular particle can be placed into the focus (under computer control) so that single particle spectroscopy and photobleaching kinetics measurements can be performed.

A laser power of 260 μ W (measured at the sample) was employed in obtaining the single molecule image of Figure 2. The fluorescence detection efficiency was determined to be 5~7%, using dye-loaded nanospheres (Invitrogen) as standards. Typical single particle fluorescence count rates of 25 kHz were observed. Analysis of fluorescence spots in the single molecule image (Figure 2) yields an estimate of the full-width at half-maximum of around 450 nm, somewhat above the diffraction limit. Improved resolution could be achieved by spatial filtering the output of the Ti:Sapphire laser. 4 Based on the determined focal characteristics of the laser and the two-photon action cross-section (2.0×10⁴ GM for ~10 nm nanoparticle), it is estimated that $\sim 32 \,\mu\text{W}$ average power (at the sample) would be required to attain this 25 kHz signal level (assuming 100 fs pulses and 6% detection efficiency). This factor of 8 discrepancy is reasonable given that there are a number of factors that are difficult to quantify and were not taken into account, such as group velocity dispersion resulting in stretched pulses, non-ideal beam profile, and non-optimal alignment. The observed modest intensity requirements for multiphoton imaging raise the possibility of employing CW excitation for multiphoton imaging. Based on these results, it is estimated that CW excitation power as low as ~10 mW (at the sample) would

be adequate for two-photon excited fluorescence detection and imaging of single CP dot particles. Such powers are readily obtained using small, inexpensive near IR diode lasers.

References for the supporting information

- 1. Xu, C.; Webb, W. W., J. Opt. Soc. Am. B 1996, 13, 481.
- Szymanski, C.; Wu, C.; Hooper, J.; Salazar, M. A.; Perdomo, A.; Dukes, A.; McNeill, J. D., *J. Phys. Chem. B* 2005, 109, 8543.
- 3. Wu, C.; Szymanski, C.; McNeill, J., Langmuir 2006, 22, 2956.
- 4. Sanchez, E. J.; Novotny, L.; Holtom, G. R.; Xie, X. S., J. Phys. Chem. A 1997, 101, 7019.

Complete author list of reference 7 in the paper

Albota, M.; Beljonne, D.; Bredas, J. L.; Ehrlich, J. E.; Fu, J. Y.; Heikal, A. A.; Hess, S. E.; Kogej, T.; Levin, M. D.; Marder, S. R.; McCord-Maughon, D.; Perry, J. W.; Rockel, H.; Rumi, M.; Subramaniam, C.; Webb, W. W.; Wu, X. L.; Xu, C., *Science* **1998**, 281, 1653.

Complete author list of reference 17 in the paper

Rumi, M.; Ehrlich, J. E.; Heikal, A. A.; Perry, J. W.; Barlow, S.; Hu, Z. Y.; McCord-Maughon, D.; Parker, T. C.; Rockel, H.; Thayumanavan, S.; Marder, S. R.; Beljonne, D.; Bredas, J. L., *J. Am. Chem. Soc.* **2000**, 122, 9500